Transaldolase is essential for maintenance of the mitochondrial transmembrane potential and fertility of spermatozoa

Andras Perl*†‡, Yueming Qian*, Kazim R. Chohan§, Cynthia R. Shirley¶, Wendy Amidon*, Sanjay Banerjee*, Frank A. Middleton‖, Karina L. Conkrite*, Maureen Barcza§, Nick Gonchoroff§, Susan S. Suarez**, and Katalin Banki§

Departments of *Medicine, †Microbiology and Immunology, §Pathology, and ‖Neuroscience and Physiology, College of Medicine, State University of New York, Syracuse, NY 13210; ¶Murine Cryopreservation Laboratory, University of California, Davis, CA 95616; and **Department of Biomedical Sciences, College of Veterinary Medicine, Cornell University, Ithaca, NY 14853

Edited by Ryuzo Yanagimachi, University of Hawaii, Honolulu, HI, and approved July 27, 2006 (received for review April 2, 2006)

Fertility of spermatozoa depends on maintenance of the mitochondrial transmembrane potential ($\Delta\psi_m$), which is generated by the electron-transport chain and regulated by an oxidation–reduction equilibrium of reactive oxygen intermediates, pyridine nucleotides, and glutathione (GSH). Here, we report that male mice lacking transaldolase (TAL)$^{-/-}$ are sterile because of defective forward motility. TAL$^{-/-}$ spermatozoa show loss of $\Delta\psi_m$ and mitochondrial membrane integrity because of diminished NADPH, NADH, and GSH. Mitochondria constitute major Ca^{2+} stores; thus, diminished mitochondrial mass accounts for reduced Ca^{2+} fluxing, defective forward motility, and infertility. Reduced forward progression of TAL-deficient spermatozoa is associated with diminished mitochondrial reactive oxygen intermediate production and Ca^{2+} levels, intracellular acidosis, and compensatory down-regulation of carbonic anhydrase IV and overexpression of CD38 and γ-glutamyl transferase. Microarray analyses of gene expression in the testis, caput, and cauda epididymidis of TAL$^{+/+}$, TAL$^{+/-}$, and TAL$^{-/-}$ littermates confirmed a dominant impact of TAL deficiency on late stages of sperm-cell development, affecting the electron-transport chain and GSH metabolism. Stimulation of *de novo* GSH synthesis by oral *N*-acetyl-cysteine normalized the low fertility rate of TAL$^{+/-}$ males without affecting the sterility of TAL$^{-/-}$ males. Whereas TAL$^{-/-}$ sperm failed to fertilize TAL$^{+/+}$ oocytes *in vitro*, sterility of TAL$^{-/-}$ sperm was circumvented by intracytoplasmic sperm injection, indicating that TAL deficiency influenced the structure and function of mitochondria without compromising the nucleus and DNA integrity. Collectively, these data reveal an essential role of TAL in sperm-cell mitochondrial function and, thus, male fertility.

Forward motility and fertility of spermatozoa depend on production of reactive oxygen intermediates (ROIs) (1) and maintenance of the mitochondrial transmembrane potential ($\Delta\psi_m$) (2, 3). $\Delta\psi_m$ is generated by the electron-transport chain and subject to regulation by an oxidation–reduction equilibrium of ROI, pyridine nucleotides (NADH/NAD + NADPH/NADP), and reduced glutathione (GSH) (4). In turn, NADPH, a reducing equivalent required for biosynthetic reactions and regeneration of GSH from its oxidized form, is produced by the pentose phosphate pathway (PPP) (5). The PPP was originally formulated based on metabolites and enzymes detected in yeast (6). Thus, PPP comprises two separate oxidative and nonoxidative phases. Enzymes of the oxidative phase, glucose 6-phosphate dehydrogenase (G6PD) and 6-phosphogluconate dehydrogenase, can generate both ribose 5-phosphate (R5P) and NADPH. Although enzymes of the nonoxidative phase, transketolase (TK) and transaldolase (TAL), can convert R5P into glucose 6-phosphate (G6P) for the oxidative phase, and, thus, indirectly, these enzymes can also contribute to the generation of NADPH, the significance of the nonoxidative branch is less well established. Certain organisms (7, 8) and mammalian tissues do not express TAL (9), and, significantly, the nonoxidative phase can be formulated without this enzyme (10); therefore, the overall reason for existence of TAL had not been established.

To investigate the role of TAL in the PPP and mammalian development in general, the genomic locus was inactivated in the mouse. Here, we report that TAL$^{-/-}$ mice develop normally; however, males are sterile because of functional and structural defects of mitochondria.

Results

Inactivation of the Mouse TAL (TAL-M) Gene Locus by Homologous Recombination. We replaced a 1,116-bp EcoRI-PstI fragment harboring adjacent parts of exon 4 and intron 4 of the TAL-M locus with the *neo* gene (Fig. 7*A*, which is published as supporting information on the PNAS web site). This manipulation deleted amino acid residues 138–153, including lysine 142, which is essential for catalytic activity of TAL (11). The 129SvJ-derived TC1 ES cells heterozygous for the disrupted allele were microinjected into C57BL/6 blastocysts to generate chimeras. Chimeric males were mated with C57BL/6 females, and tail DNA of the offspring was tested for transmission of the targeted allele by PCR (Fig. 7*B*), Southern blot (Fig. 7*C*), and Western blot analyses (Fig. 7*D*). Among 692 pups born to heterozygote parents, the proportion of WT (168 of 692, 24.4%), heterozygote (355 of 692, 51.2%), and homozygote knockout genotypes (169 of 692, 24.4%) followed the expected Mendelian inheritance.

Complete Male Infertility in Homozygous and Partial Male Infertility in Heterozygous Knockout Mice. Breeding pairs were set up between adult (>8 weeks of age) male and female mice born to different heterozygote parents. TAL$^{+/-}$ males had reduced fertility, and TAL$^{-/-}$ males were completely infertile (Fig. 1). Although vaginal plugs were observed, 15 TAL$^{-/-}$ males paired with WT females produced no pregnancy over 5 months. TAL$^{-/-}$ males displayed no obvious differences in weight and development. Weight and light-microscopic morphology of their reproductive organs (testes, sem-

Author contributions: A.P., Y.Q., K.R.C., C.R.S., and K.B. designed research; A.P., Y.Q., W.A., K.R.C., C.R.S., S.B., F.A.M., K.L.C., M.B., N.G., S.S.S., and K.B. performed research; A.P., Y.Q., W.A., K.R.C., C.R.S., S.B., F.A.M., S.S.S., and K.B. analyzed data; and A.P. and K.B. wrote the paper.

The authors declare no conflict of interest.

This paper was submitted directly (Track II) to the PNAS office.

Abbreviations: CAIV, carbonic anhydrase IV; $\Delta\psi_m$, mitochondrial transmembrane potential; G6PD, glucose 6-phosphate dehydrogenase; GGT, γ-glutamyl transpeptidase; GSH, glutathione; ICSI, intracytoplasmic sperm injection; NAC, *N*-acetyl cysteine; PPP, pentose phosphate pathway; ROI, reactive oxygen intermediate; S7P, sedoheptulose 7-phosphate; TAL, transaldolase; TK, transketolase.

Data deposition: The sequence reported in the paper has been deposited in the GenBank database (accession no. AY466103).

‡To whom correspondence should be addressed at: Department of Medicine, State University of New York, 750 East Adams Street, Syracuse, New York 13210. E-mail: perla@upstate.edu.

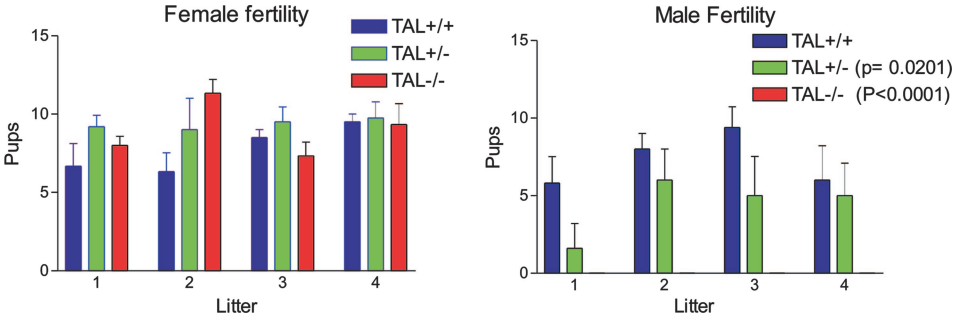

Fig. 1. Male infertility in TAL-deficient mice. Fifteen male and 15 female mice of each genotype were paired, with a single WT female or male per cage. Values indicate mean number ± SD of pups per breeding pair recorded for four generations. Based on comparison with $TAL^{+/+}$ controls, *P* values <0.05 are shown.

inal vesicles, prostate, and epididymis) did not differ from those of $TAL^{+/-}$ and $TAL^{+/+}$ littermates. Sperm of all developmental stages were present in similar numbers in the testes and efferent ducts. Complete or partial TAL deficiency did not influence female fertility (Fig. 1).

Diminished Forward Motility and *in Vitro* Fertility of TAL-Deficient Spermatozoa. The motility of spermatozoa was investigated by using a computer-assisted semen-analysis system. Although no significant differences were observed in total numbers and viability of spermatozoa, motility parameters, including progressive velocity (straight line velocity) and track speed were markedly reduced, whereas beat frequency of $TAL^{-/-}$ sperm was increased (Table 1). Tracings of video images revealed stiffened flagellar midpieces of $TAL^{-/-}$ sperm (Fig. 8, which is published as supporting information on the PNAS web site). We attempted to rescue infertility of $TAL^{-/-}$ sperm by *in vitro* fertilization. Sperm of four $TAL^{-/-}$ mice failed to fertilize oocytes from 8-week-old $TAL^{+/+}$ females. By contrast, sperm of four control $TAL^{+/+}$ littermates fertilized oocytes and resulted in development of blastocysts (Fig. 9, which is published as supporting information on the PNAS web site). Infertility of $TAL^{-/-}$ sperm was rescued by intracytoplasmic sperm injection (ICSI). Injection of sperm from the caput or cauda epididymidis of $TAL^{-/-}$ mice into oocytes led to blastocyst development (Table 2, which is published as supporting information on the PNAS web site). Blastocysts from $TAL^{+/+}$ or $TAL^{-/-}$ sperm gave rise to similar numbers of pups, indicating that infertility of $TAL^{-/-}$ males was rescued by ICSI.

Loss of $\Delta\psi_m$, Diminished Mitochondrial ROI Production, Reduced Cytoplasmic and Mitochondrial Ca^{2+} Levels, and Intracellular Acidification in TAL-Deficient Sperm Cells. Mitochondria play crucial roles in spermatogenesis and sperm motility (12). Therefore, $\Delta\psi_m$ of $TAL^{+/+}$, $TAL^{+/-}$, and $TAL^{-/-}$ spermatozoa was comparatively analyzed by using potentiometric fluorescent dyes TMRM, $DiOC_6$, and JC-1. Sperm viability was monitored by parallel staining with annexin V-PE or annexin V-FITC (13, 14) matched with emission spectra of potentiometric-, oxidation-, or Ca^{2+}-sensitive fluorescent probes (15, 16). Although overall viability of $TAL^{-/-}$, $TAL^{+/-}$, or $TAL^{+/+}$ spermatozoa was not different, $\Delta\psi_m$ of $TAL^{-/-}$ spermatozoa was profoundly diminished (Fig. 2 and Fig. 10, which is published as supporting information on the PNAS web site). $\Delta\psi_m$ of $TAL^{+/-}$ spermatozoa was reduced to a lesser extent. Mitochondrial mass in $TAL^{-/-}$ spermatozoa was diminished, as determined by NAO and MTG fluorescence. The extent of $\Delta\psi_m$ loss, as determined by $DiOC_6$ fluorescence, exceeded the loss of mitochondrial mass detected by NAO and MTG fluorescence. Reduced JC-1 FL-2/FL-1 fluorescence also suggested loss of $\Delta\psi_m$ independent of mitochondrial mass.

Maintenance of $\Delta\psi_m$ is required for generation of ROI (17); thus, reduced $\Delta\psi_m$ may lead to diminished ROI production by TAL-deficient sperm cells. As shown in Fig. 2, ROI levels, monitored by dihydroethidium (hydroethidine, DHE) as well as by dihydrorhodamine and dichlorofluorescein (data not shown) (15), were diminished in $TAL^{+/-}$ and $TAL^{-/-}$ sperm. As monitored by monochlorobimane fluorescence, intracellular thiol content, largely composed of GSH, was diminished in $TAL^{-/-}$, but not $TAL^{+/-}$, spermatozoa.

Intracellular Ca^{2+} is essential for normal motility of sperm cells (18). As shown in Figs. 2 and 10, intracytosolic Ca^{2+} levels, as determined by Fluo-3 fluorescence and, in particular, mitochondrial Ca^{2+} levels, as determined by Rhod-2 fluorescence, were profoundly reduced, which may account for increased beat frequency and diminished forward motility of $TAL^{-/-}$ spermatozoa. Rhod-2, but not Fluo-3, fluorescence was also significantly reduced in $TAL^{+/-}$ spermatozoa, suggesting that lower mitochondrial Ca^{2+} levels may be primarily responsible for reduced fertility of $TAL^{+/-}$ males (Fig. 1). The acrosome reaction, a Ca^{2+}-dependent process, was also reduced in $TAL^{-/-}$ sperm and, to a lesser extent, in $TAL^{+/-}$ cells (data not shown). With respect to WT cells, intracellular pH was reduced in $TAL^{+/-}$ and $TAL^{-/-}$ spermatozoa (Figs. 2 and 10).

Structural Abnormalities of Mitochondria in $TAL^{-/-}$ Spermatozoa. Phase-contrast (data not shown) and bright-field microscopy showed no structural abnormalities in sperm cells isolated from cauda epididymidis of $TAL^{+/-}$ or $TAL^{-/-}$ mice. However, fluorescence microscopy revealed profoundly diminished $DiOC_6$ staining of the mitochondrial midsection in $TAL^{-/-}$ spermatozoa and, to a lesser extent, in $TAL^{+/-}$ spermatozoa (Fig. 3*A*), in accordance with flow-cytometry studies (Fig. 2). Because NAO and MTG fluorescence also indicated an overall reduction of mitochondrial-membrane mass, the internal structure of the mitochondria was examined by EM. As expected (19), mitochondria were arranged in a cylinder-shaped sheath that wrapped around the axial outer dense fiber–axoneme complex of the midpiece (Fig. 3*B*). Although the outer mitochondrial membranes were appropriately retained, the internal membrane structure of the mitochondria was irregular, with disappearance of cristae-like folds and formation of electron-dense central clumps in $TAL^{-/-}$ spermatozoa (Fig. 3*B*). Similar changes were observed in sperm cells in the caput and cauda

Table 1. Motility analysis of spermatozoa from $TAL^{+/+}$, $TAL^{+/-}$, and $TAL^{-/-}$ mice

Parameter	$TAL^{+/+}$	$TAL^{+/-}$	$TAL^{-/-}$
Motile, %	45.3 ± 7.8	42.7 ± 7.9 (n.s.)	24.6 ± 7.5 (0.004)
Path velocity, μm/s	105.000 ± 8.9	72.6 ± 8.2 0.0183)	37.6 ± 8.8 (0.0052)
Progressive velocity, μm/s	51.3 ± 0.3	43.8 ± 0.6 (0.0070)	33.0 ± 0.5 (0.0012)
Track speed, μm/s	193.6 ± 17.9	139.8 ± 26.6 (0.0069)	90.8 ± 36.6 (0.0026)
Beat frequency, Hz	23.0 ± 1.2	27.6 ± 1.3 (0.0203)	30.6 ± 1.9 (0.0074)

Spermatozoa were isolated from cauda epididymidis, and 100–200 cells of each specimen were characterized by using an automated Hamilton–Thorne Research sperm analyzer. Data represent mean ± SE, based on analysis of six mice from each genotype. Sperm with progressive motility >11 μm/s were considered motile. *P* values (in parentheses) reflect comparison with $TAL^{+/+}$ samples. n.s., not significant.

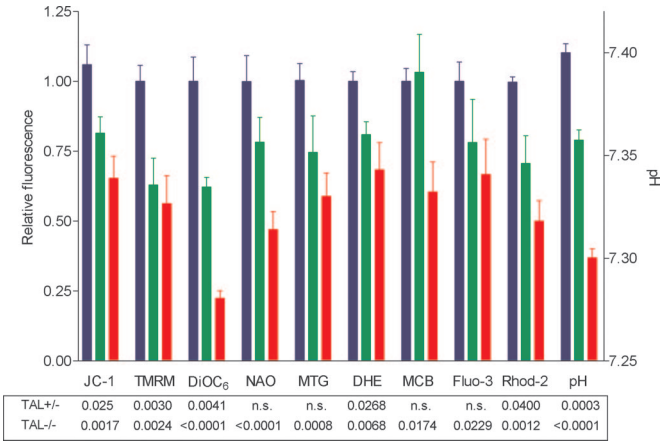

Fig. 2. Cumulative assessment of $\Delta\psi_m$, mitochondrial mass, ROI, GSH, and cytoplasmic and mitochondrial Ca^{2+} levels in live spermatozoa from $TAL^{+/+}$, $TAL^{+/-}$ and $TAL^{-/-}$ littermates. Results were expressed as relative fluorescence values with respect to those of $TAL^{+/+}$ cells normalized at 1.0 on the left *y* axis. Absolute pH values based on SNARF-1 fluorescence of calibration standards are shown on the right *y* axis. Data present mean ± SE of eight independent experiments. *P* values under each column reflect comparison of $TAL^{+/-}$ (green) and $TAL^{-/-}$ (red) spermatozoa to $TAL^{+/+}$ (blue) ones. n.s., not significant.

epididymidis but not in the testis of $TAL^{-/-}$ mice. The head of the spermatozoa was of normal size and shape, and the tail section exhibited the expected pattern of two central microtubules, surrounded by nine tubules and a set of outer dense fibers.

Accumulation of Sedoheptulose 7-Phosphate (S7P) and Depletion of Pyridine Nucleotides in TAL-Deficient Tissues. To investigate the metabolic bases of mitochondrial dysfunction in TAL deficiency, phosphorylated sugar metabolites of the PPP and pyridine nucleotides were measured by HPLC. Complete TAL deficiency resulted in marked accumulation of S7P in testis of $TAL^{-/-}$ mice (Fig. 4*A*). S7P is a substrate of the forward reaction of TAL that generates glucose 6-phosphate for NADPH production by enzymes of the oxidative phase of the PPP (Fig. 11, which is published as supporting information on the PNAS web site). NADPH and NADH levels were diminished in $TAL^{-/-}$ and, to a lesser extent, in $TAL^{+/-}$ cauda epididymidis (Fig. 4*B*), suggesting a dominant role for TAL in the generation of these reducing equivalents by the PPP. NAD, ADP-ribose, AMP, cAMP, ADP, and ATP were diminished only in $TAL^{-/-}$ cauda epididymidis (Fig. 4*B*). Diminished NADH levels were consistent with the tendency to maintain NADPH at the expense of NADH by transhydrogenases (20). Depletion of ATP by 59.9% in $TAL^{-/-}$ ($P = 0.0029$), but not in $TAL^{+/-}$, spermatozoa with respect to those $TAL^{+/+}$ littermates was independently confirmed by using the luciferin–luciferase assay. ATP depletion may have resulted from the damage of mitochondria, which are estimated to provide as much as 90% of ATP in the sperm (21). However, sperm cells of mice lacking the sperm-specific isozyme of glyceraldehyde 3-phosphate dehydrogenase also show dysmotility and reduced ATP without mitochondrial damage (22). These findings suggest that mitochondrial ATP synthesis alone may not be responsible for sperm dysmotility. Indeed, *in vitro* addition of cell-permeable cAMP analogues cAMP-acetoxymethyl ester and dibutyryl cAMP (23), NADPH (1), or ATP, by using up to 500 μM each nucleotide, failed to enhance motility of $TAL^{-/-}$ or $TAL^{+/-}$ spermatozoa (data not shown).

TAL Deficiency-Induced Changes of Gene Expression Are Confined to the Cauda Epididymidis and Affect Mitochondrial Function, Ca^{2+} Signaling, and Pathways Involved in Sperm Motility. To investigate the impact of TAL deficiency on signaling pathways involved in

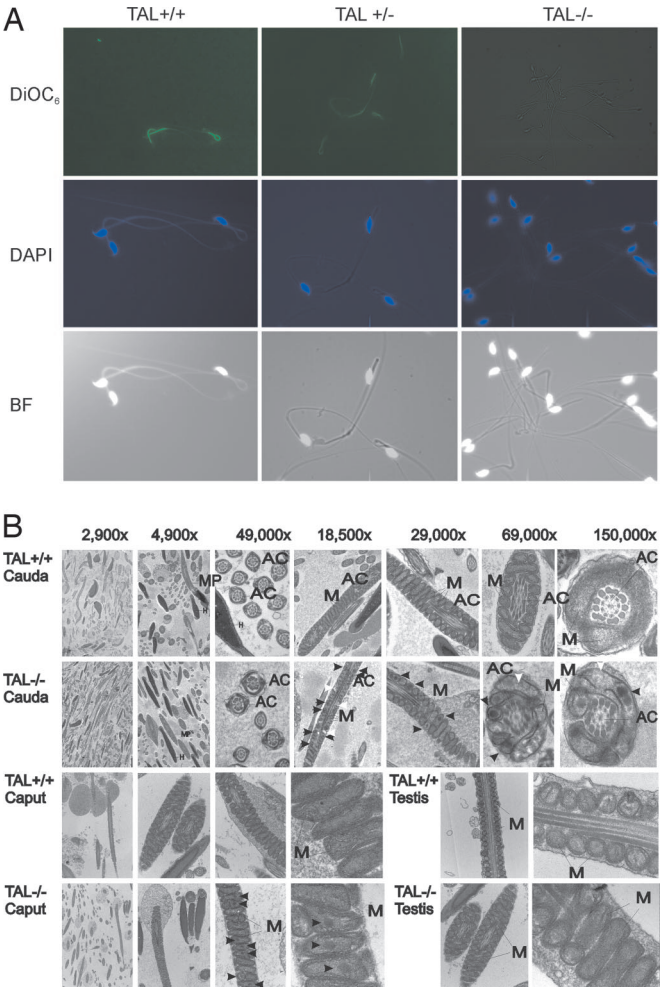

Fig. 3. Loss of $\Delta\psi_m$ and structural changes in mitochondria of TAL-deficient sperm. (*A*) Fluorescence microscopy of spermatozoa from $TAL^{+/+}$, $TAL^{+/-}$, and $TAL^{-/-}$ mice. Cells were stained with $DiOC_6$ (green) and DAPI (blue) to detect $\Delta\psi_m$ of mitochondria in the midsection and DNA in heads of sperm cells, respectively. BF, bright-field images. With respect to $TAL^{+/+}$ sperm, $\Delta\psi_m$ was progressively diminished in $TAL^{+/-}$ and $TAL^{-/-}$ sperm. (Magnification, ×400.) (*B*) Transmission EM of cauda and caput epididymidis and testis from $TAL^{+/+}$ and $TAL^{-/-}$ littermate mice. Original magnification is shown above images of cauda epididymidis. Mitochondria (M) are arranged in a cylinder-shaped sheath that wraps spirally around the axial outer dense fiber–axoneme complex of the midpiece (MP). No structural defects were observed in the head and tail section of $TAL^{-/-}$ spermatozoa. The head (H) was of normal size and shape. The axoneme complex (AC) of $TAL^{-/-}$ sperm showed the expected pattern of two central microtubules, surrounded by nine tubules, intact dynein arms, and a set of outer dense fibers. Although the outer mitochondrial membranes were appropriately retained, the internal membrane structure of mitochondria was irregular, with disappearance of cristae-like folds (white arrows) and formation of electron-dense central clumps in mitochondria of $TAL^{-/-}$ spermatozoa in cauda and caput epididymidis (black arrows).

sperm motility, microarray and subsequent quantitative real-time RT-PCR analyses were performed on RNA from testis and caput and cauda epididymidis. Expression of 511 of 22,690 genes was increased or decreased by >2-fold in $TAL^{+/-}$ or $TAL^{-/-}$ tissues in comparison with $TAL^{+/+}$ controls. As shown in the heat color diagrams (Fig. 12, which is published as supporting information on the PNAS web site), most genes altered by TAL deletion are differentially expressed between testis and caput and cauda epididymidis, suggesting involvement in sperm-cell maturation. The most profound changes were noted in cauda epididymidis of $TAL^{-/-}$ mice, where expression of 483 genes was increased or

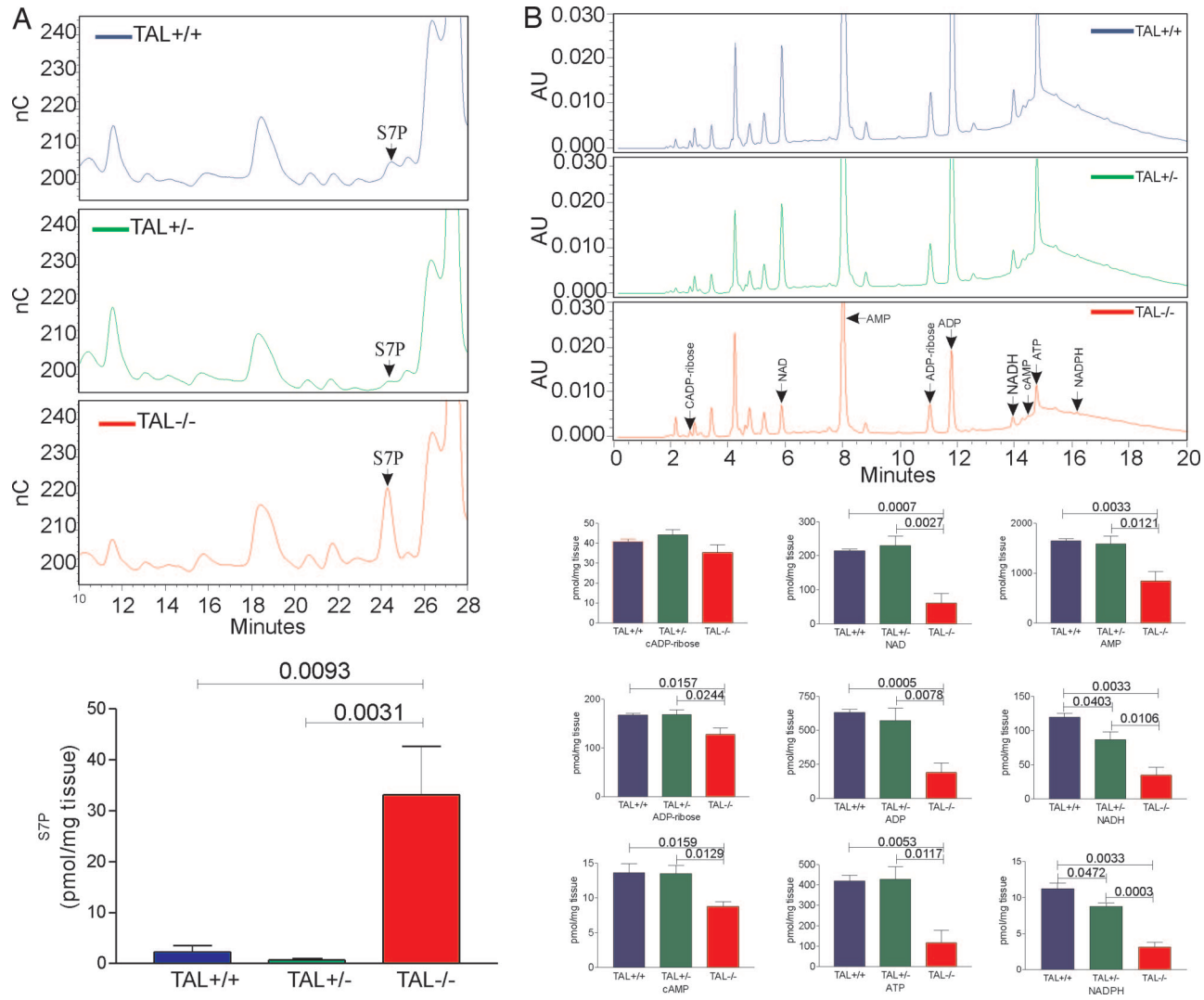

Fig. 4. HPLC analysis of PPP sugars and nucleotides. (*A*) HPLC analysis of S7P in testis of TAL$^{+/+}$, TAL$^{+/-}$, and TAL$^{-/-}$ mice. Chromatograms indicate electric charge (nanocoulomb) of sugar phosphates recorded on a pulse amperometric detector. S7P was positively identified by spiking TAL$^{+/+}$ tissue extract with sugar phosphate standard (data not shown). Bar charts show comparative analysis of S7P levels in testis from age-matched TAL$^{+/+}$, TAL$^{+/-}$, and TAL$^{-/-}$ littermates. Data show mean ± SE of measurements from four mice per genotype. *P* values <0.05 reflect differences between genotypes. (*B*) Analysis of nucleotides in cauda epididymidis of TAL$^{+/+}$, TAL$^{+/-}$, and TAL$^{-/-}$ mice by HPLC. Chromatograms indicate UV absorbance (AU). Annotated peaks were positively identified by spiking TAL$^{+/+}$ tissue extracts separately with each compound (data not shown). Bar charts show comparative analysis of nucleotide levels in tissues from age-matched TAL$^{+/+}$, TAL$^{+/-}$, and TAL$^{-/-}$ littermates. Data show mean ± SE of measurements from four mice per genotype. *P* values <0.05 are indicated.

decreased by >2-fold. Similar changes affected only 84 and 4 genes in caput epididymidis and testis, respectively, of TAL$^{-/-}$ mice. Coordinate changes were noted in expression of genes of the PPP and interconnected metabolic pathways, the electron-transport chain, and other mitochondrial proteins, gene expression, apoptosis, adhesion and immune function, ion transport, GSH metabolism and redox signaling, nucleotide metabolism, Ca^{2+} signaling, and development and motility of spermatozoa (Fig. 12). With a focus on genes involved in sperm motility (24), quantitative real-time RT-PCR analyses confirmed altered expression of γ-glutamyl transpeptidase (GGT), GSH peroxidase, calmodulin, calmodulin-dependent cyclic nucleotide phosphodiesterase, Soggy1, sperm-specific lactate dehydrogenase, and carbonic anhydrase IV (CAIV). Changes in CAIV, CD38, and GGT expression may represent a complementary mechanism involved in male infertility of TAL$^{-/-}$ mice. Of note, CAIV has been implicated in regulating intracellular pH of spermatozoa (25, 26). Transcription of CAIV was increased 4.02-fold ($P = 3.5 \times 10^{-6}$) in TAL$^{+/-}$ cauda epididymidis, whereas it was undetectable in TAL$^{-/-}$ cauda epididymidis by real-time RT-PCR. As documented by Western blot analysis, CAIV protein levels were increased in TAL$^{+/-}$ cauda epididymidis by 82 ± 18% ($P = 0.011$) and profoundly reduced in cauda epididymidis of TAL$^{-/-}$ mice (−76 ± 3.5%, $P < 0.001$; Fig. 5*A*). In agreement with microarray data, expression of CD38 or NAD hydrolase was increased on the surface of TAL$^{-/-}$ spermatozoa (Fig. 5*B*). As a control (Fig. 10*F*), CD59 expression was reduced on the surface of TAL$^{-/-}$ spermatozoa (Fig. 5*B*).

TAL protein and activity levels were halved in TAL$^{+/-}$ testis, epididymis, and spermatozoa, and they were undetectable in TAL$^{-/-}$ tissues (Fig. 5*C*). Activities of PPP enzymes G6PD and TK were unchanged in these TAL$^{+/-}$ and TAL$^{-/-}$ tissues. GSH was reduced in TAL$^{-/-}$ spermatozoa (Fig. 2), indicating that profound NADPH depletion affected regeneration of GSH from its oxidized form, GSSG. Whereas NADPH was reduced, GSH levels were normal in TAL$^{+/-}$ spermatozoa, suggesting compensatory changes in *de novo* synthesis or salvage of GSH. Activity of GGT, an ectoenzyme involved in GSH salvage, was increased in both TAL$^{+/-}$ and TAL$^{-/-}$ cauda epididymidis (Fig. 5*C*).

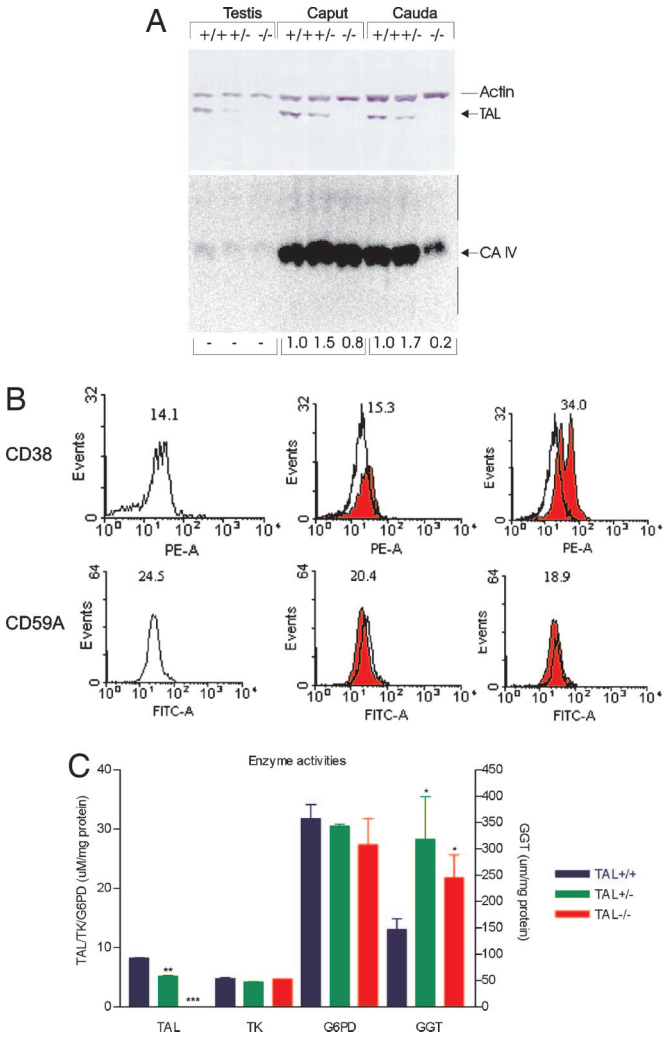

Fig. 5. Effect of TAL deficiency on expression of CAIV, CD38, and GGT. (*A*) Western blot analysis of CAIV expression in testis and caput and cauda epididymidis of $TAL^{+/+}$, $TAL^{+/-}$, and $TAL^{-/-}$ littermates. Blots were first developed with rabbit antibody to CAIV then reexposed to antibodies to TAL and actin. By using automated densitometry, CAIV expression levels in each tissue were normalized to actin levels and compared with $TAL^{+/+}$ cells set at 1.0. (*B*) Expression of CD38 on the surface of sperm cells from $TAL^{+/+}$, $TAL^{+/-}$, and $TAL^{-/-}$ littermates gated on live cells based on forward scatter and side scatter. Antibody to CD59 was used as a control. Histograms of $TAL^{+/-}$ and $TAL^{-/-}$ spermatozoa (shaded curves) are overlayed on those from $TAL^{+/+}$ littermate controls (open curves). Data represent analysis of five experiments. (*C*) Activity of TAL, TK, G6PD (left *y* axis), and GGT (right *y* axis) in cauda epididymidis of $TAL^{+/+}$, $TAL^{+/-}$, and $TAL^{-/-}$ mice. Data represent mean ± SD of four sets of $TAL^{+/+}$, $TAL^{+/-}$, and $TAL^{-/-}$ littermates. *, $P < 0.05$; **, $P < 0.01$; ***, $P < 0.0001$.

Interestingly, both male and female GGT-deficient mice are infertile, and their fertility can be restored by stimulation of *de novo* GSH synthesis with *N*-acetyl cysteine (NAC) (27). After weaning at 3 weeks of age, 10 g/liter NAC was added to the drinking water of male littermates. At the age of 3 months, breeding pairs were set up between $TAL^{+/+}$, $TAL^{+/-}$, or $TAL^{-/-}$ male littermates, six of each genotype, and age-matched $TAL^{+/-}$ female littermates and given NAC in the drinking water. Oral NAC treatment normalized the $\Delta\psi_m$, mitochondrial mass, mitochondrial and cytosolic Ca^{2+} levels, and ROI production of $TAL^{+/-}$ sperm (data not shown). Whereas $TAL^{-/-}$ males produced no pregnancies, $TAL^{+/+}$ and $TAL^{+/-}$ males produced 15 ± 1.9 and 16 ± 2.9 pups, respectively, over a period of 60 days. Thus, NAC normalized the fertility of $TAL^{+/-}$ males without affecting the sterility of $TAL^{-/-}$ males.

Discussion

The present data show that TAL plays a critical role in male fertility through the maintenance of the $\Delta\psi_m$ and structural integrity. TAL is an enzyme of the nonoxidative phase of the PPP, which generates two major products, (*i*) NADPH for biosynthetic reactions and maintenance of a reducing environment and (*ii*) ribose 5-phosphate for synthesis of nucleotides (Fig. 11). The medical importance of PPP was first appreciated when partial G6PD deficiency was associated with hemolytic anemia (28). G6PD has been uniformly regarded as the rate-controlling enzyme of the PPP (5). Targeted disruption of the G6PD gene in mouse ES cells showed a complete lack of survival of homozygous knockout cells (29). Likewise, mouse embryos with complete TK deficiency were not viable. $TK^{+/-}$ mice exhibited general growth retardation (−35%) and a similar reduction in gonadal mass and the number of pups born to $TK^{+/-}$ females (30). These results indicated that G6PD and TK play essential housekeeping roles in cellular metabolism (29). By contrast, $TAL^{+/-}$ or $TAL^{-/-}$ mice developed normally and exhibited no reduction in weight or lifespan at 1 year of age.

The role of TAL in the functioning of the PPP and metabolism in general has been poorly understood. The PPP has been formulated with and without TAL, and, indeed, organisms lacking TAL have been documented (7, 8). Enzymatic activity (31–37) and expression of TAL is regulated in a tissue-specific manner (9, 38–40). TAL catalyzes the transfer of a three-carbon fragment, corresponding to dihydroxyacetone, from S7P and fructose 6-phosphate to D-glyceraldehyde 3-phosphate and D-erythrose 4-phosphate in the forward and reverse reactions, respectively (Fig. 11). In the absence of TAL, S7P, a substrate of the forward TAL reaction accumulated >7-fold in testis, urine, and liver (data not shown) from $TAL^{-/-}$, but not $TAL^{+/-}$, mice. Accumulation of S7P is compatible with a failure to recycle ribose 5-phosphate into glucose 6-phosphate through the nonoxidative phase of the PPP, thus, reducing NADPH production by G6PD and 6-phosphogluconate dehydrogenase (Fig. 11). Indeed, NAPDH levels were reduced in cauda epididymidis of $TAL^{+/-}$ or $TAL^{-/-}$ mice (Fig. 4*B*).

Male infertility affects as much as 10% of the adult population. Most cases are characterized by a reduced or absent movement of spermatozoa of unknown etiology (41). The present data reveal a critical role for TAL in NADPH production and maintenance of $\Delta\psi_m$ and motility of spermatozoa. Whereas $TAL^{-/-}$ sperm failed to fertilize $TAL^{+/+}$ oocytes *in vitro*, the fertility of $TAL^{-/-}$ sperm was rescued by ICSI. These results indicated that TAL deficiency selectively impacted the structure and function of mitochondria without affecting the nucleus and DNA integrity. Thus, this study clearly identifies TAL deficiency as a cause of sperm dysmotility and male infertility.

Materials and Methods

Development of TAL-Deficient Mice. Cloning of the mouse TAL (TALDO1) genomic locus, construction of the TALDO1 targeting vector, homologous recombination and generation of germ-line chimeras, and testing of WT ($TAL^{+/+}$), heterozygote ($TAL^{+/-}$), and homozygote ($TAL^{-/-}$) offspring by PCR, Southern blot hybridization, and Western blot analysis are described in *Supporting Methods*, which is published as supporting information on the PNAS web site.

Microarray and Quantitative Real-Time Reverse-Transcriptase-Mediated PCR Analysis of Gene Expression. See *Supporting Methods*.

Enzyme Activity Assays. TAL, TK, G6PD, and GGT activities were determined as described (42, 43).

Assessment of Fertility. Littermate males (>8 weeks of age) were separated and paired with females (>8 weeks of age) for 5 months or more. The number of mice achieving pregnancy and the number of offspring from each breeding pair and pregnancy were recorded.

Sperm-Motility Analysis. The cauda epididymidis was excised, placed into 5 ml of Sperm Washing Medium (Irvine Scientific, Santa Ana, CA), and minced, and dispersed sperm cells were separated from solid tissue remnants by passing through a 70-μm cell strainer (Becton Dickinson, Franklin Lakes, NJ). Sperm movement was quantified within 30 min after removal from animals by a computer-assisted semen-analysis system (IVOS version 12, Hamilton–Thorne Research, Beverly, MA).

Flow Cytometry. $\Delta\psi_m$, mitochondrial mass, ROI production, GSH, cytoplasmic and mitochondrial Ca^{2+} level, intracellular pH, and acrosome reaction were analyzed by flow cytometry, as described in the *Supporting Methods*.

HPLC and Mass Spectrometry. Measurement of PPP sugar metabolites and nucleotides by HPLC and tandem mass spectrometry is described in *Supporting Methods*.

ATP Measurement by Chemiluminescence. Intracellular ATP levels were determined by using the luciferin–luciferase method (44).

Video Microscopy. Motility of live spermatozoa was observed on a Zeiss Axioskop microscope under stroboscopic dark-field illumination at flash rates between 50 and 150 Hz and recorded with a Sony (Tokyo, Japan) AVC-D7 video camera (Movie 1, which is published as supporting information on the PNAS web site).

Immunofluorescence Microscopy. For fluorescence microscopy, sperm cells were resuspended in Sperm Refrigeration Medium (Irvine Scientific) and stained with 40 nM $DiOC_6$ (green) and 1 μM DAPI (blue) to detect $\Delta\psi_m$ of mitochondria in the midsection and DNA in heads of sperm cells. Specimen were examined with a Zeiss Axioskop 2 microscope equipped with a Hamamatsu (Hamamatsu City, Japan) OCRA-ER digital camera.

EM. Freshly excised tissues were fixed overnight in PBS with 2.5% glutaraldehyde, postfixed in 1% OsO_4, dehydrated in graded ethanol series, infiltrated with propylene oxide, and embedded in Araldite 502 epoxy resin. Ultrathin sections were stained with uranyl acetate and Reynold's lead citrate before examination under a Tecnai BioTWIN 12 transmission electron microscope (FEI, Hillsboro, OR).

***In Vitro* Fertilization (IVF) and ICSI.** IVF (45) and ISCI were performed, as described in the *Supporting Methods* (46–48).

Statistics. Results were analyzed by Student's t test or Mann–Whitney rank-sum test for nonparametric data. Correlation was measured by using Pearson's correlation coefficient. Changes were considered significant at $P < 0.05$.

We thank Dr. Paul Phillips for continued encouragement and support; Drs. Steven Grassl, Michael Lieberman, David Mitchell, and Gary Olson for helpful discussions; Dr. William Sly (St. Louis University, St. Louis, MO) for providing antibody to carbonic anhydrase; and Michael Hillman for technical assistance. This work was supported by National Institutes of Health Grant R01 DK49221.

1. Fisher HM, Aitken RJ (1997) *J Exp Zool* 277:390–400.
2. Marchetti C, Obert G, Deffosez A, Formstecher P, Marchetti P (2002) *Hum Reprod* 17:1257–1265.
3. Marchetti C, Jouy N, Leroy-Martin B, Defossez A, Formstecher P, Marchetti P (2004) *Hum Reprod* 19:2267–2276.
4. Perl A, Gergely, P, Jr, Puskas F, Banki K (2002) *Antiox Redox Signal* 4:427–443.
5. Mayes PA (1993) in *Harper's Biochemistry*, eds Murray RK, Granner DK, Mayes PA, Rodwell VW (Appleton & Lange, Norwalk, CT), pp 201–211.
6. Horecker BL, Mehler AH (1955) *Annu Rev Biochem* 24:207–274.
7. Susskind BM, Warren LG, Reeves RE (1982) *Biochem J* 204:191–199.
8. Feldmann SD, Sahm H, Sprenger GA (1992) *Appl Microbiol Biotechnol* 38:354–361.
9. Grossman CE, Qian Y, Banki K, Perl A (2004) *J Biol Chem* 279:12190–12205.
10. Wood T (1972) *FEBS Lett* 25:153–155.
11. Banki K, Perl A (1996) *FEBS Lett* 378:161–165.
12. Bourgeron T (2000) in *The Genetic Basis of Male Infertility*, ed McElreavey K (Springer, Berlin; Heildelberg) pp 187–210.
13. Paasch U, Sharma RK, Gupta AK, Grunewald S, Mascha EJ, Thomas AJ, Jr, Glander HJ, Agarwal A (2004) *Biol Reprod* 71:1828–1837.
14. Maeda Y, Shiratsuchi A, Namiki M, Nakanishi Y (2002) *Cell Death Differ* 9:742–749.
15. Banki K, Hutter E, Gonchoroff N, Perl A (1999) *J Immunol* 162:1466–1479.
16. Nagy G, Koncz A, Perl A (2003) *J Immunol* 171:5188–5197.
17. Stryer L (1988) *Biochemistry* (Freeman, New York).
18. Suarez SS, Varosi SM, Dai X (1993) *Proc Natl Acad Sci USA* 90:4660–4664.
19. Olson GE, Winfrey VP (1992) *Mol Reprod Dev* 33:89–98.
20. Rydstrom J (1977) *Biochim Biophys Acta* 463:155–184.
21. Meinhardt A, Wilhelm B, Seitz J (1999) *Hum Reprod Update* 5:108–119.
22. Miki K, Qu W, Goulding EH, Willis WD, Bunch DO, Strader LF, Perreault SD, Eddy EM, O'Brien DA (2004) *Proc Natl Acad Sci USA* 101:16501–16506.
23. Esposito G, Jaiswal BS, Xie F, Krajnc-Franken MAM, Robben TJAA, Strik AM, Kuil C, Philipsen RLA, van Duin M, Conti M, *et al.* (2004) *Proc Natl Acad Sci USA* 101:2993–2998.
24. Matzuk MM, Lamb DJ (2002) *Nat Cell Biol* 4:S33–S40.
25. Kaunisto K, Fleming RE, Kneer J, Sly WS, Rajaniemi H (1999) *Biol Reprod* 61:1521–1526.
26. Ekstedt E, Holm L, Ridderstrale Y (2004) *J Mol Histol* 35:167–173.
27. Kumar TR, Wiseman AL, Kala G, Kala SV, Matzuk MM, Lieberman MW (2000) *Endocrinology* 141:4270–4277.
28. Cooper RA, Bunn HF (1991) in *Harrison's Principles of Internal Medicine*, eds Wilson JD, Braunwald E, Isselbacher KJ, Petersdorf RG, Martin JB, Fauci AS, Root RK (McGraw–Hill, New York) pp 1531–1543.
29. Pandolfi PP, Sonati F, Rivi R, Mason P, Grosveld F (1995) *EMBO J* 14:5209–5215.
30. Xu ZP, Wawrousek EF, Piatigorsky J (2002) *Mol Cell Biol* 22:6142–6147.
31. Novello F, McLean P (1968) *Biochem J* 107:775–791.
32. Heinrich PC, Morris HP, Weber G (1976) *Cancer Res* 36:3189–3197.
33. Severin SE, Stepanova NG (1981) *Adv Enzyme Regul* 19:235–255.
34. Wood T (1985) *The Pentose Phosphate Pathway* (Academic, New York).
35. James HM, Williams SG, Bais R, Rofe AM, Edwards JB, Conyers RAJ (1985) *Int J Vitam Nutr Res* Suppl 28:29–46.
36. Kauffman FC, Harkonen MHA (1977) *J Neurochem* 28:745–750.
37. Hothersall JS, Baquer NZ, McLean P (1982) *Enzyme* 27:259–267.
38. Banki K, Colombo E, Sia F, Halladay D, Mattson D, Tatum A, Massa P, Phillips PE, Perl A (1994) *J Exp Med* 180:1649–1663.
39. Baquer NZ, Hothersall JS, McLean P, Greenbaum AL (1977) *Dev Med Child Neurol* 19:81–104.
40. Thom E, Mohlman T, Quick WP, Camara B, Neuhaus HE (1998) *Planta* 204:226–233.
41. Acacio BD, Gottfried T, Israel R, Sokol RZ (2000) *Fertil Steril* 73:595–597.
42. Banki K, Hutter E, Colombo E, Gonchoroff NJ, Perl A (1996) *J Biol Chem* 271:32994–33001.
43. Lachaise F, Martin G, Drougard C, Perl A, Vuillaume M, Wegnez M, Sarasin A, Daya-Grosjean L (2001) *Free Radical Biol Med* 30:1365–1373.
44. Gergely PJ, Niland B, Gonchoroff N, Pullmann, R, Jr, Phillips PE, Perl A (2002) *J Immunol* 169:1092–1101.
45. Summers MC, Bhatnagar PR, Lawitts JA, Biggers JD (1995) *Biol Reprod* 53:431–437.
46. Kimura Y, Yanagimachi R (1995) *Biol Reprod* 52:709–720.
47. Shirley CR, Hayashi S, Mounsey S, Yanagimachi R, Meistrich ML (2004) *Biol Reprod* 71:1220–1229.
48. Li MW, McGinnis L, Zhu L, Lawitts J, Biggers J, Lloyd KC (2003) *Comp Med* 53:265–269.
49. Masters BA, Kelly EJ, Quaife CJ, Brinster RL, Palmiter RD (1994) *Proc Natl Acad Sci USA* 91:584–588.
50. Banki K, Halladay D, Perl A (1994) *J Biol Chem* 269:2847–2851.